Available online at www.sciencedirect.com

ScienceDirect

Energy Procedia 97 (2016) 334 – 341

Energy Procedia

European Geosciences Union General Assembly 2016, EGU
Division Energy, Resources & Environment, ERE

The geothermal field below the city of Berlin, Germany: Results from structurally and parametrically improved 3D Models

Maximilian Frick[a,b,*], Judith Sippel[a], Mauro Cacace[a], Magdalena Scheck-Wenderoth[a,c]

[a] *Section 6.1: Basin Analysis, GFZ German Research Centre for Geosciences, Telegrafenberg, 14473 Potsdam, Germany*
[b] *Freie Universitt Berlin, Institute of Geological Sciences, Malteserstr. 74-100, 12249 Berlin, Germany*
[c] *RWTH Aachen, School of Geosciences, Templergraben 55, 52056 Aachen, Germany*

Abstract

The objective of this study is to analyze the influence of geological structure and parameterization of Cenozoic sediments on the geothermal field as calculated by 3D thermohydraulic numerical simulations for the subsurface of Berlin, Germany. The results show, that a mostly continuous Rupelian aquitard effectively hampers forced convective cooling of the deep subsurface ($\geq 1km$) but for localities where the unit is discontinuous. New parameterization methods for hydraulic conductivities lead to a stronger coupling of the hydraulic boundary condition and forced convective cooling. Newly derived thermal conductivities result in a stronger thermal blanketing effect for the Post-Permian sediments than previously estimated.

Peer-review under responsibility of the organizing committee of the General Assembly of the European Geosciences Union (EGU)

Keywords: 3D geological model; Coupled fluid and heat transport; Sensitivity analysis; Boundary conditions; Urban future; Geothermal energy

1. Introduction

Understanding the present-day thermal and hydraulic configuration below major urban centers (e.g. Berlin) situated in sedimentary basins becomes increasingly more important as renewable energy resources (e.g. geothermal energy) contribute to reducing CO_2-emissions [1]. Hence, understanding the different coupled physical processes involved and their interrelation with the respective parameters is essential even with respect to possible future model scenarios (e.g. anthropogenic forcing). The major contributors to the thermal field are diffusion of heat by conduction and convective heat transport driven by circulating groundwater. The latter can include topography-driven flow, overpressure flow, or flow induced by buoyant forces within the fluid. Each of these processes and their respective effect on the present-day geothermal field is mainly controlled by the local hydrogeological setting which is represented in new detail in this study.

Despite a relatively flat topography (Fig. 1a) and no recent tectonic activity in the Northeast German Basin, latest 3D numerical investigations of coupled fluid and heat transport indicate a regional hydrothermal regime which

* Corresponding author. Tel.: +49-331-288-2828
E-mail address: mfrick@gfz-potsdam.de

Peer-review under responsibility of the organizing committee of the General Assembly of the European Geosciences Union (EGU)
doi:10.1016/j.egypro.2016.10.011

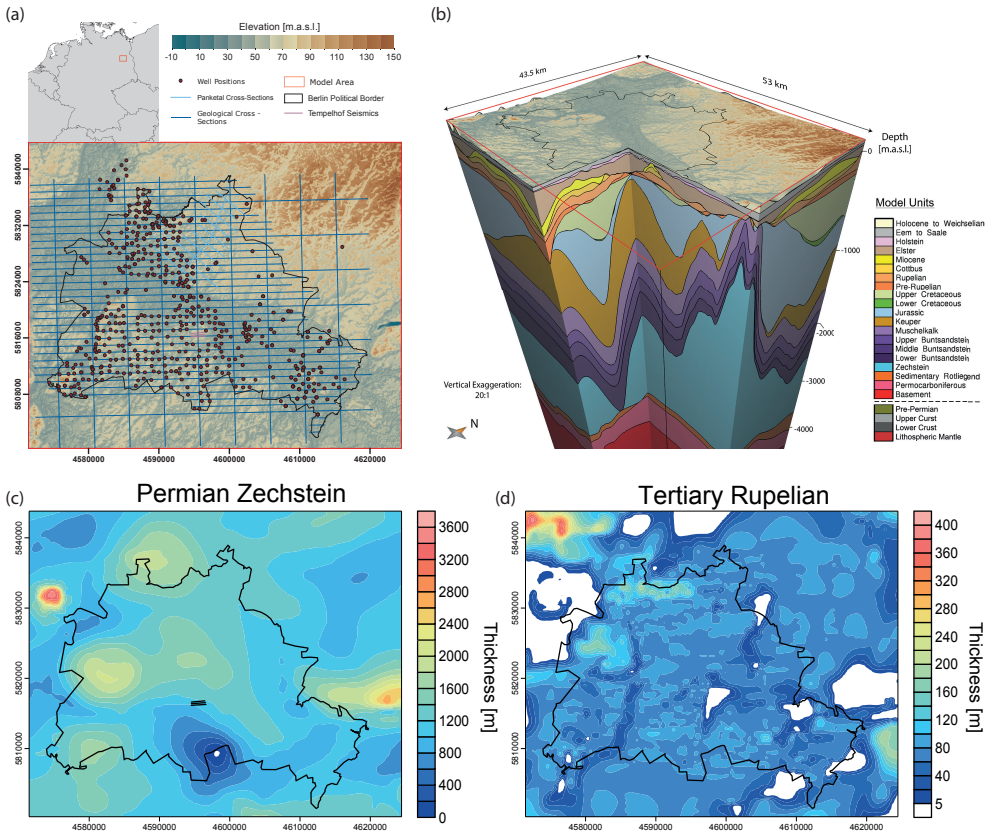

Fig. 1. Database and new structural model of the subsurface of Berlin, Coordinates are in Gauß-Krüger DHDN Zone 4. Black line indicates political border of Berlin. (a) Location of the model area in central Europe and database (b) 3D structural model as used for all thermal simulations. Depicted on top is the elevation distribution of the uppermost layer (see a). Model units and vertical extent of models for the different modeling methods as indicated in Section 3. (c) Thickness distribution of the Permian Zechstein salt unit. Black lines in the center indicate the location of the Tempelhof seismics, (d) Thickness distribution of the Oligocene Rupelian clay. (c,d) White areas represent discontinuities. Database provided by Senate Department for Urban Development and the Environment of Berlin (SenStadtUm) and Berlin waterworks (BWB).

is largely influenced by conductive heat transport additionally overprinted by a regional component of pressure (topographically) driven groundwater flow extending to variable depths [2,3]. Predicted temperatures reproduce the available measured borehole temperature measurements only to a certain degree showing a local and systematic misfit. This misfit is predominantly evident at shallower depth levels (< 3km), where modeled temperatures are generally colder than measured values. Two different causes for the observed discrepancies have been suggested [2]: (1) a lack of accuracy in representing the surface thermal and hydraulic boundary conditions, (2) insufficiently detailed representation and diversification of the shallow Tertiary and Quaternary aquifer complexes.

This study is part of ongoing activities aiming at investigating and quantifying the relative impact of the aforementioned parameters on the present-day thermal configuration of the subsurface of Berlin, capital city of Germany. The objective of the three models run (M1-3), is to analyze the influence of the geological structure and the model unit parameterization on the geothermal field. Since model units physical parameters like thermal or hydraulic conductivities are rarely well constrained by measured data, we opt in a new method, where we parameterized youngest model units in accordance with their lithological and/or grain size distributions (see Section 3). We followed a two-step approach where (1) a new structural model has been built according to newly available data, (2) Numerical thermal and hydraulic simulations have been carried out based on (1) (see Sections 2 and 4).

2. Geological Setting and Structural Model

The first step of this study was the construction of a new structural model of the study area by utilizing newly available data mainly focusing on the shallow Paleogene and Neogene aquifer system. Local deep seismics at Tempelhof were also implemented and cover strata down to Permian times. The database (Fig. 1a) included 57 geological cross-sections, more than 600 well logs (both limited to the shallow model domain, > -400 m.a.s.l.), three local deep seismic profiles (< -4000 m.a.s.l.), which have been integrated into an existing structural model (vertical extent down to Lithosphere-Asthenosphere-Boundary (LAB), [2] and the references cited therein). This 3D information on the structural configuration of the Berlin subsurface was compiled, visualized and interpolated with the commercial software package Petrel (© Schlumberger). The data were integrated into a consistent 3D structural model differentiating 18 units (8 Cenozoic units) for the sedimentary basin fill (Fig. 1b) and 5 units for the underlying basement, namely Permocarboniferous Volcanics, Pre-Permian, Upper Crust, Lower Crust and Lithospheric Mantle. The purely conductive Model (see Sections 3 and 4) covers all geological units down to the LAB, whereas the coupled models have been limited in vertical extent, reaching down to a depth of -6000 m.a.s.l., thus integrating all 18 sedimentary units overlying the volcanics.

The sedimentary succession ranges from Permian to Cenozoic in age and consists predominantly of clastics, carbonates and rock salt [4]. The latter is mainly found in the Permian Zechstein unit which significantly controlled and modified the geometry of the post salt succession (mobilization of Zechstein salt from Middle Triassic times onward [5]). It has locally increased thicknesses of more than 3400 m and shows a complex topological configuration (Fig. 1c). The implementation of the new data led to changes in the thickness distribution in the Tempelhof area of up to 230 m, visualized in the complete withdrawal of the Zechstein salt (discontinuity) in the S (Fig. 1c). The remaining Mesozoic sediments are mainly composed of consolidated clastics or carbonates [4]. This succession also includes two geological units of special interest for geothermal applications, namely the Middle Triassic (Middle Buntsandstein) and Permian Sedimentary Rotliegend, which consist of sandstones consolidated to varying degrees and with a porosity and permeability high enough to be considered as potential target horizons for geothermal installations beneath Berlin [6]. The overlying younger Cenozoic sediments, represented by 8 model units ([2]: 6), are predominantly composed of unconsolidated clastics (Fig. 2) which contain the main shallow fresh water aquifer system for water supply of Berlin. Of these eight units, the most important modification compared to the most recent model [2] relates to the interbedded local aquitard of the Rupelian clay, which is more continuous in the structural model constructed in this study (Fig. 1d). It also shows zero thickness only at a few locations, most prominently in the NW and E, coinciding with thickness maxima of the Zechstein at these locations. Thus, the Rupelian aquitard separates the upper fresh water aquifers and the lower saline aquifers more effectively and continuously [7] connecting the two compartments only locally. With these results, the new structural model shows, that the sediments of the Rupelian were deposited more continuously and eroded (e.g. through incision of glacial channels [2]) much less drastically than previously assumed [2] with an average thickness of $\approx 66\,m$ ($\approx 40\,m$ in [2]).

3. Modeling Method and Scenarios

3.1. Purely Conductive Heat Transport (M1)

The purely conductive thermal simulations run in this study utilize the assumption that the main heat transport mechanism in the Earth's lithosphere is conduction. Under the assumption of thermal equilibrium (i.e. steady-state, $\frac{\partial T}{\partial t} = 0$) this process can be described by:

$$\nabla \cdot (\lambda^{(b)} \nabla T) = S \tag{1}$$

with ∇ = nabla operator, $\lambda^{(b)}$ = bulk thermal conductivity, T = temperature and S = radiogenic heat production.

From Eq. (1) follows, that calculated subsurface temperatures depend only on radiogenic heat production, bulk thermal conductivity and the boundary conditions (BC) chosen. The 3D numerical computation of the purely conductive thermal field was carried out with GMS [4] implementing the structural model described in Section 2. For this purpose each model unit was assigned a constant value for λ and S (Table 1, see Section 3.3). This model scenario

implements 23 geological units down to the LAB as a base for the coupled simulations in order to consider the heat input from the deep subsurface ($d_{max} = -129,604\,m.a.s.l.$).

Table 1. Properties of the model units as used for the thermal calculations. Properties of Cretaceous and older units after [2]. $\lambda^{(b)}$ = bulk thermal conductivity, S = radiogenic heat production, $c^{(s)}$ = heat capacity of solid, ϕ = porosity, κ = hydraulic conductivity; M2, M3 = Model 2, 3. Values were derived from [2,8–13].

	Geological unit	$\lambda^{(b)}$ [$W/m*K$]	S [$\mu W/m^3$]	$c^{(s)}$ [$kJ/kg*K$]	ϕ [−]	κ M2 [m/s]	κ M3 [m/s]
Neogene	Holocene to Weichselian	2.71	0.9	1.57	0.32	9.62E-08	1.42E-05
	Eemian to Saalian	2.59	0.9	1.58	0.314	9.62E-08	4.04E-06
	Holstein	2.17	0.9	1.67	0.296	9.62E-08	1.91E-08
	Elsterian	2.35	0.9	1.61	0.304	9.62E-08	8.98E-07
	Miocene	2.47	1.0	1.56	0.301	9.62E-08	6.88E-07
Paelog.	Cottbus	2.62	1.3	1.7	0.305	9.62E-08	1.15E-06
	Rupelian	1.64	1.3	1.81	0.237	impermeable	3.23E-08
	Pre-Rupelian	2.48	1.3	1.7	0.297	9.62E-08	6.56E-07

3.2. Coupled Fluid and Heat Transport (M2, M3)

For the coupled heat and fluid simulations, the 3D geological model was imported into the commercial software FEFLOW©[14]. The latter solves for (un)saturated groundwater flow in porous media taking into account conductive, advective and buoyant (fluid-density related) heat transport processes within a finite element based computational framework. Details about the mathematical background and its numerical formulation can be found in [14]. Model units were populated with values for thermal conductivity (λ), volumetric heat capacity (c), radiogenic heat production (S), porosity (ϕ) and hydraulic conductivity (K, Table 1, see Section 3.3).

The horizontal resolution of the models is 100x100 m. To guarantee a good vertical to horizontal element shape ratio the original 20 geological units (Fig. 1b) with distinct physical properties were further subdivided, so that the final structural model is composed of 56 computational layers (at least two per geological unit).

Due to the high non-linearity of the coupled problem, models were run in transient state for both, fluid and heat transport, until reaching quasi-steady-state conditions which is assumed to be reached after a maximum of $10^8\,days\,(\approx 250\,kyrs)$ final simulation time. Initial time step length was set to $10^{-3}\,d$ and the maximum time step length was $5x10^4\,d$.

3.3. Model Unit Parameterization

Since no new information on physical properties of the Pre-Cenozoic succession were available, these model units are defined by the same parameterization as in [2]. To determine the physical properties of the Cenozoic succession, the petrological information provided along with the well data from SenStadtUm and BWB was used. Each stratigraphic unit was analyzed for its lithological distribution weighted over the cumulative thickness of all wells (Fig. 2). The lower threshold for considering a lithology in this analysis was chosen to be ≥0.5% of each individual lithology per stratigraphic unit.

To finalize the parameterization, the lithological distributions of each Cenozoic model unit were combined with published data of the physical properties [8,9,11,12,15–20]. Consequently, lithology distribution depended averaged isotropic values for thermal conductivity, heat capacity and porosity were assigned to each model unit. An exception to this approach was made for the hydraulic conductivities (M2, M3). In the first coupled scenario (M2), the latter were defined by the values used in [2] (Table 1). In contrast, M3 utilized a grain size distribution based approach presented in [13]. The latter allows to use grain size distributions derived from the well database for each geological unit as quasi sieve-experiment to derive hydraulic conductivities after common formulae (e.g. Cozeny-Carmen, Hazen). The values derived this way are combined using the arithmetic mean of those passing the validity test (i.e. Schlichter: 0.01 cm < d_{10} (diameter of $10^{th}\,weight-\%ile$) < 0.5 cm, more details in [13]). This arithmetic mean was assigned to all Cenozoic units individually whereas major changes in comparison to M2 are generally higher hydraulic conductivities, a lowly permeable Rupelian clay (M2: impermeable) and the differentiation of the Neogene Holstein as another lowly

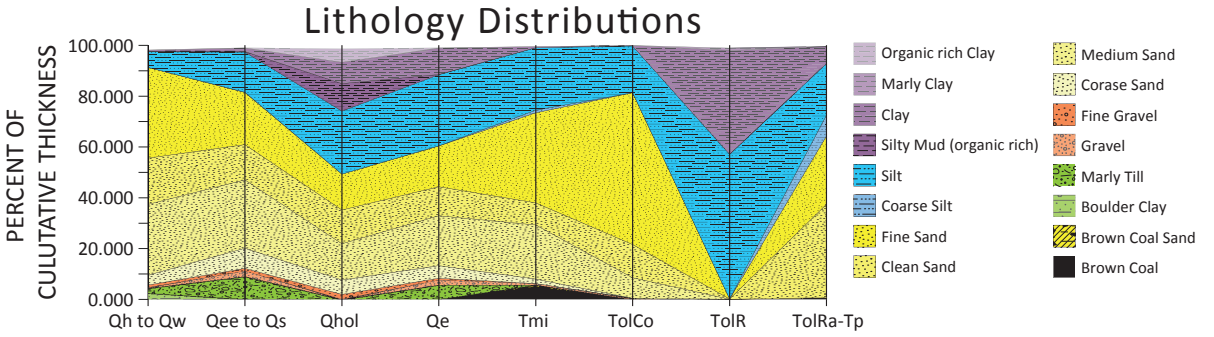

Fig. 2. Lithological distribution as derived from well logs. Grain Size decreases from top to bottom (bottom-most four excluded). Qh = Holocene, Qw = Weichselian, Qee = Eemian, Qs = Saalian, Qhol = Holstein, Qe = Elsterian, Tmi = Miocene, TolCo = Cottbus, TolR = Rupelian, TolRa = Sands of the Base of the Rupelian, Tp = Paleocene.

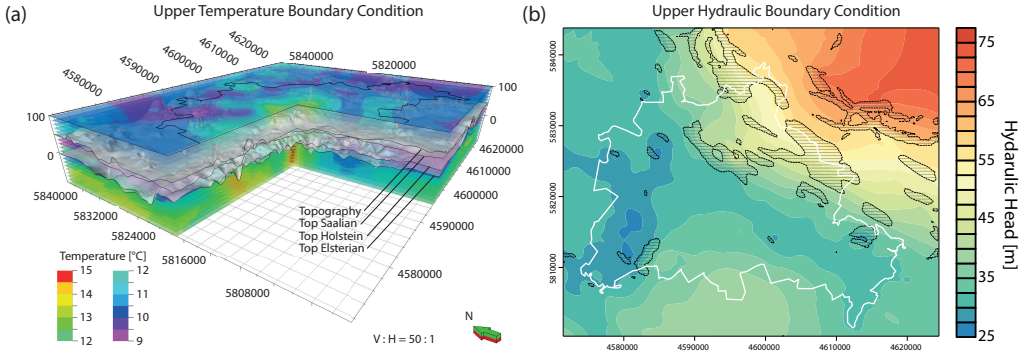

Fig. 3. Upper thermal and hydraulic BC. Coordinates are in Gauß-Krüger DHDN Zone 4. (a) Upper thermal BC viewed in 3D, derived from temperature measurements reaching from + 90 m.a.s.l. to - 100 m.a.s.l. (b) Upper hydraulic BC as derived from groundwater level measurements, hatched areas represent regions with high hydraulic potential.

permeable local aquitard (Table 1, [7]). With this approach, the lack of measured in situ data of a physical property (e.g. hydraulic conductivity) might be bridged by utilizing available codependent physical properties (e.g. grain size distribution) to derive the missing parameter. Consequently, this method could also be used for different codependent physical properties, supposedly favoring the less erroneous, more easily available or the one with better coverage over the model area. Herein, the possibility of laterally variable physical parameterization instead of isotropic average values for model units arises.

3.4. Boundary and Initial Conditions

In order to solve the mathematical problem, thermal and hydraulic upper and lower BC are required. Firstly, all lateral boundaries are closed to both, fluid and heat flow. Newly available measured temperature data (partly utilized in [21]) have been implemented as upper thermal BC after 3D interpolation. In detail, the heterogeneous temperature distribution (Min: 9 °C, Max: 15 °C) was assigned to the top surfaces of all Quaternary units (Holocene, Saalian, Holstein, Elster, Fig. 3a, [22]). Thereby, highest temperatures are located below the city centers of Berlin and Potsdam (likely connected to surface sealing, [7]) and lower temperatures are found beneath rural areas (Fig. 3a).

The lower temperature BC in the conductive model (M1) uses the general approach of the LAB representing the depth where the mantle adiabat cuts the geotherm corresponding to the solidus of mantle peridotite which lies at the 1300 °C isotherm [2]. In comparison, the coupled models (M2, M3) utilized the conductively calculated temperature of M1 at - 6000 m.a.s.l. as the respective lower thermal BC (see Section 4, Fig. 4b).

Additionally, the coupled models utilize measured groundwater levels (= hydraulic heads) as the upper hydraulic BC (Fig. 3b). Here, highest elevations are located in the NE (Barnim Plate) and S (Teltow Plate) while lowest

elevations follow the greater Spree river valley striking SE-NW. Areas with a high hydraulic potential are mostly located at the border between the greater Spree river valley and the Barnim Plate and within the latter (Fig. 3b).

The purely conductive simulation was run in steady state. To calculate temperature and pressure initial conditions of the coupled model simulations, the different scenarios were run for decoupled fluid and heat transport in steady state conditions.

4. Model Results and Discussion

The temperatures predicted by the purely conductive simulation (M1) at -6000 m.a.s.l. range from 196.6 °C in the NW gradually increasing to 220.5 °C in the SE (Fig. 4b). These results show, that the thermal field at this depth is mainly controlled by the radiogenic heat input from the upper crust below ($S = 2.3 \frac{\mu W}{m^3}$, [2]), which shows a thickness distribution gradually increasing from NW to SE [2]. At -1000 m.a.s.l. temperatures range from 42.8 °C to 52.4 °C (Fig. 4a) with maxima correlating with highest thicknesses of the Permian Zechstein (Fig. 1c) and vice versa as already demonstrated in earlier studies [2–4,23]. However, predicted temperatures of this study are generally higher in comparison with earlier modeling efforts (e.g.[2] at -6000 m.a.s.l.: T_{min} = 188.9 °C, T_{max} = 216,4 °C) which may be attributed to three parameters: (1) more continuous Rupelian (lowest thermal conductivity Table 1, Fig. 1d), (2) a general drop in thermal conductivity of Cenozoic succession (2.38 $\frac{W}{m*K}$ Table 1, [2]: 3.16 $\frac{W}{m*K}$) and (3) an increase in temperature of the upper thermal BC (Fig. 3a). The first two of those lead to an increase in the thermal blanketing effect exerted by the post-Zechstein succession which can be observed even at large depths (e.g. T_{diff_max} = +7.9°C at -6000 m.a.s.l. compared to [2] Model A). In contrast, the newly implemented upper temperature BC has only a limited effect restricted to shallow levels, most prominently visible in an increase of predicted temperatures below the city center of Berlin (Fig. 3a, Fig. 4a).

Model scenarios 2 and 3 are used to quantify the influence of the new structural model on coupled heat transport and testing the sensitivity of the models to different model unit hydraulic conductivities for the Cenozoic succession. Model 2 predicts temperatures ranging from 41.0 °C to 51.5 °C (mean: 45.4 °C) at -1000 m.a.s.l. which is generally colder than those predicted by Model 1. Temperature differences range between +1.6 °C and -3.7°C with a mean of -1.1 °C (Fig. 4c). Maximum differences between predicted temperatures are very localized, correlating with areas of high or low hydraulic potential Fig. 4c). Additionally, these areas almost exclusively associate with discontinuities of the Rupelian aquitard (hydrogeological windows, Fig. 4c). Consequently, these results are likely caused by over-pressured infiltration of cold surface water into the deeper model domain via discontinuities in the Rupelian aquitard, driven by existing hydraulic gradients. This finding is in accordance with earlier modeling efforts [2,21]. However, the magnitude of the induced cooling is significantly reduced (T_{diff_max} = -22.7 °C; -11.3 °C at -1000 m.a.s.l. in [2];[21]), which is likely connected with (1) a more continuous Rupelian clay aquitard preventing the infiltration of cold surface water and (2) utilizing measured groundwater levels as hydraulic boundary condition [21]. However, (1) relies on the assumption of a completely impervious Rupelian clay, which makes (2) more influential as outlined below.

The sensitivity of the models to different hydraulic conductivities of the Cenozoic ($\kappa_{M2} < \kappa_{M3}$) is investigated in the last model scenario (M3). Predicted temperatures at -1000 m.a.s.l. range from 35.9 °C to 50.5 °C, with a mean value of 43.8 °C. In comparison with the purely conductive model scenario (Model 1) this translates to maximum differences of -8.4 °C to +1.0 °C (mean: -2.8 °C, Fig. 4d). These temperatures are also in general colder than those calculated for M2 (T_{diff_max} = -7.0 °C). Maximum differences are mainly located in areas displaying a high hydraulic potential while little to no difference is predicted in areas of low hydraulic potential (Fig. 4d). These findings suggest, that in an environment of forced convective heat transport, gradients in the hydraulic BC are likely high enough to cause leakage of cold surface water through the Rupelian into the Pre-Rupelian succession. M3 also locally predicts higher temperatures than M2 which might be indicative for a general change of fluid dynamics in the system opening the possibility of rising heated water from below the Rupelian leaking upwards. This would present a potential source for salinization of the shallow fresh water aquifers, which is a common problem in the NEGB (e.g. [24]).

In comparison to measured temperatures at the observation wells (1) *Gt Berlin-Wartenberg 2/86* and (2) *Gt Velten 2/90*, the coupled models show a good fit ((1): $dT_{av}M2$ = 0.23 °C, (2) $dT_{av}M3$ = 0.79 °C, Fig. 4e). Especially at shallow depths (structurally most improved, see Section 2), measured and modeled absolute temperatures and temperature gradients could be reproduced comparatively accurately [2]. At higher depths (>1000 MD) deviations between measured and modeled values increase as small wavelength variations in the geothermal gradient cannot be

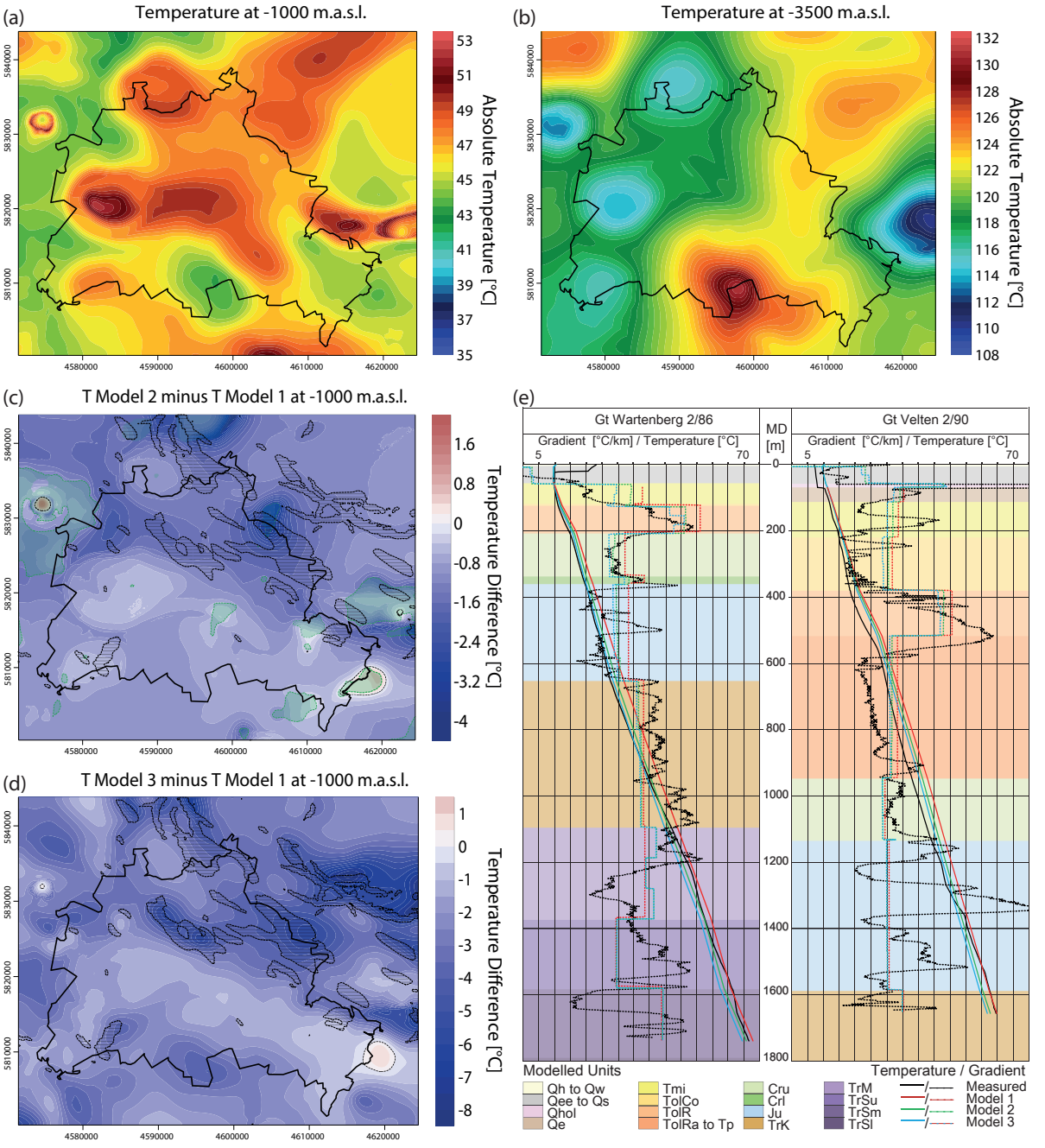

Fig. 4. Model results for the different model scenarios. Coordinates are in Gauß-Krüger DHDN Zone 4. (a) Predicted temperatures for Model 1 at -1000 m.a.s.l. (b) -6000 m.a.s.l. (c) Temperature differences between Model 2 and 1 at -1000 m.a.s.l., shaded green areas represent discontinuities in the Rupelian aquitard, (d) Temperature differences between Model 3 and 1 at -1000 m.a.s.l., (c,d) Dashed areas represent high hydraulic potential (e) Measured and modeled Temperatures at *Gt Berlin-Wartenberg 2/86* and *Gt Velten 2/90*, MD = measured depth, Qh = Holocene, Qw = Weichselian, Qee = Eemian, Qs = Saalian, Qhol = Holstein, Qe = Elsterian, Tmi = Miocene, TolCo = Cottbus, TolR = Rupelian, TolRa = Sands of the Base of the Rupelian, Tp = Paleocene, Cru = Upper Cretaceous, Crl = Lower Cretaceous, Ju = Jurassic, TrK = Keuper, TrM = Muschelkalk, TrSu = Upper Buntsandstein, TrSm = Middle Buntsandstein, TrSl = Lower Buntsandstein.

reproduced by the current geological model. This misfit is likely a derivative of a insufficiently detailed representation of Pre-Rupelian model units due to a lack of available data concerning lithological distributions and measured physical properties. Therefore, a reliable validation of model results based on the sparsely available measured temperature data is not possible at this point of time. Hence, ongoing studies focus on the implementation of groundwater recharge rates, surface water bodies, groundwater wells and solute transport as additional parameters to overcome this obstacle.

Acknowledgments

We would like to thank the Senate Department for Urban Development and the Environment of Berlin (SenStadtUm) and Berlin waterworks (BWB) for providing the data for this study.

References

[1] Bromley, C.J., Mongillo, M., Goldstein, B., Hiriart, G., Bertani, R., Huenges, E., et al. Contribution of geothermal energy to climate change mitigation: the IPCC renewable energy report. In: Proceedings World Geothermal Congress 2010. 2010,.
[2] Sippel, J., Fuchs, S., Cacace, M., Kastner, O., Huenges, E., Scheck-Wenderoth, M.. Deep 3D thermal modelling for the city of Berlin (Germany). Environmental Earth Scienes 2013;doi:10.1007/s12665-013-2679-2.
[3] Noack, V., Scheck-Wenderoth, M., Cacace, M., Schneider, M.. Influence of fluid flow on the regional thermal field: results from 3D numerical modelling for the area of Brandenburg (North German Basin). Environmental Earth Scienes 2013;doi:10.1007/s12665-013-2438-4.
[4] Bayer, U., Scheck, M., Koehler, M.. Modeling of the 3D thermal field in the northeast German basin. Geologische Rundschau 1997;86(2):241–251.
[5] Scheck, M., Bayer, U., Lewerenz, B.. Salt movement in the Northeast German Basin and its relation to major post-Permian tectonic phases - results from 3D structural modelling, backstripping and reflection seismic data. Tectonophysics 2003;361(3-4):277–299.
[6] Huenges, E., Ledru, P.. Geothermal energy systems: exploration, development, and utilization. John Wiley & Sons; 2011.
[7] Limberg, A., Thierbach, J.. Hydrostratigrafie von Berlin-Korrelation mit dem Norddeutschen Gliederungsschema. Brandenburgische Geowiss Beitr 2002;9(1):2.
[8] Otto, R.. Zur Abschätzung von Wärmeleitfähigkeiten der oberflächennahen Lockergesteinsschichtenfolge in Norddeutschland. Grundwasser 2012;17(4):219–229. doi:10.1007/s00767-012-0205-1; grundwasser.
[9] VDI, . Thermische Nutzung des Untergrundes: Grundlagen, Genehmigungen, Umweltaspekte. 2010.
[10] Norden, B., Förster, A.. Thermal conductivity and radiogenic heat production of sedimentary and magmatic rocks in the Northeast German Basin. AAPG Bulletin 2006;90(6):939–962.
[11] Norden, B., Förster, A., Behrends, K., Krause, K., Stecken, L., Meyer, R.. Geological 3-D model of the larger Altensalzwedel area, Germany, for temperature prognosis and reservoir simulation. Environmental Earth Sciences 2012;67(2):511–256.
[12] Das, B.M.. Advanced soil mechanics. CRC Press; 2013.
[13] Devlin, J.. HydrogeoSieveXL: an Excel-based tool to estimate hydraulic conductivity from grain-size analysis. Hydrogeology Journal 2015;23(4):837–844.
[14] Diersch, H.J.. FEFLOW Finite Element Subsurface Flow & Transport Simulation System, Reference Manual. Berlin: WASY GmbH Institute for Water Resources Planning and System Research; 2009.
[15] Eisermann, D.. Multi-Spezies-Modellierung sanierungsrelevanter Fragestellungen für einen heterogenen Feldstandort: SAFIRA-Bitterfeld. Ph.D. thesis; UFZ-Umweltforschungszentrum Leipzig-Halle; 2005.
[16] SenStadtUm, . 01.06 Soil-Scientific Characteristic Values (Edition 2013); vol. Berlin Environmental Atlas 2013; chap. 01 Soil. Berlin: Senate Department for Urban Development and the Environment; 2013,.
[17] Klebba, B., Gräser, S.. Kartierung potentieller Versickerungsflächen innerhalb des Berliner Stadtgebietes - Diplomkartierung. Master's thesis; Freie Universität Berlin; Berlin; 2012.
[18] Wieneke, S.. Hydrogeologische Gutachten zur Neufestsetzung von Wasserschutzgebieten im Land Brandenburg, Hinweise zur Erstellung. Fachbeiträge des Landesamtes für Umwelt, Gesundheit und Verbraucherschutz 2011;117.
[19] Haldorsen, S.. Grain-size distribution of subglacial till and its relation to glacial crushing and abrasion. Boreas 1981;10(1):91–105.
[20] Wentworth, C.K.. A scale of grade and class terms for clastic sediments. The Journal of Geology 1922;:377–392.
[21] Frick, M., Scheck-Wenderoth, M., Sippel, J., Cacace, M.. Sensitivity of a 3D Geothermal Model of Berlin with Respect to Upper Boundary Conditions. Energy Procedia 2015;76:291–300. doi:10.1016/j.egypro.2015.07.864; european Geosciences Union General Assembly 2015 - Division Energy, Resources and Environment, {EGU} 2015.
[22] SenStadtUm, . 02.14 Groundwater Temperature (Edition 2014); vol. Berlin Environmental Atlas 2014; chap. 02 Water. Berlin: Senate Department for Urban Development and the Environment; 2014,.
[23] Cherubini, Y., Cacace, M., Scheck-Wenderoth, M., Moeck, I., Lewerenz, B.. Controls on the deep thermal field: implications from 3-D numerical simulations for the geothermal research site Groß Schönebeck. Environmental earth sciences 2013;70(8):3619–3642.
[24] Magri, F., Bayer, U., Tesmer, M., Möller, P., Pekdeger, A.. Salinization problems in the NEGB: results from thermohaline simulations. International Journal of Earth Sciences 2008;97(5):1075–1085.